scientific reports

Check for updates

OPEN

Nanomagnetic picolylamine-based complex of palladium as an efficient heterogeneous catalyst for selective reduction of nitroarenes in water

Ammar Yasir Ahmed[1]✉, Hamad AlMohamadi[2,3]✉, Hazem Saed Zabibah[4], Subbulakshmi Ganesan[5], Vimal Arora[6], krithiga Thangavelu[7,11], Pusparaj Samantsinghar[8], Hamza Fadhel Hamzah[9], Basim Mohammed Saadi[9] & Yasser Fakri Mustafa[10]

In this study, a novel heterogeneous palladium complex stabilized on Fe_3O_4 magnetic nanoparticles (MNPs) was synthesized via a three-step procedure involving the functionalization of iron oxide surface with an electrophilic group (C-Cl), subsequent nucleophilic substitution reaction with 2-picolylamine, and final complexation with palladium chloride. The catalytic performance of the resulting magnetic heterostructure was then evaluated in the selective hydrogenation of nitroarenes and N-heteroarenes using $NaBH_4$ as a reducing agent. The reactions proceeded efficiently under mild, green conditions specifically, in water at room temperature to delivering the desired aniline derivatives in good to excellent yields (81–98%) within short reaction times (25–90 min). While electronic and steric factors influenced the reaction outcome, this system consistently outperformed previously reported methods in terms of both yield and reaction speed. Moreover, the catalyst exhibited exceptional stability and reusability, maintaining its structural integrity and high catalytic activity over five successive cycles without significant degradation.

Keywords [Fe_3O_4@PTMS-2-picolylamine-$PdCl_2$], Palladium complex, Hydrogenation of nitroarenes, Reduction of nitroarenes, Green chemistry, Magnetic nanocatalyst

Nitroarenes, organic compounds featuring a nitro (-NO_2) group attached to an aromatic ring, are a fascinating yet challenging class of chemicals, commonly formed through the simple nitration of aromatic compounds[1–3]. While many are known for their toxicity, exhibiting mutagenic, genotoxic, and potentially carcinogenic effects alongside their often explosive properties, their synthetic utility remains paramount[4,5]. Indeed, the reduction of these compounds is an important step in total synthesis for accessing a wide range of value-added compounds after initial nitration[6–8]. The reactivity of NO_2 group offers diverse conversion possibilities, making the development of efficient synthetic methods crucial in organic chemistry. One of the most valuable transformations is the reduction of nitroarenes to anilines[9–11]. This conversion is a cornerstone reaction, as anilines serve as vital intermediates in the creation of a vast array of products, including polymers, dyes, and pharmaceuticals. Furthermore, anilines can participate in nucleophilic reactions, be transformed into aryldiazonium salts and

[1]College of Pharmacy, University of Al Maarif, Al Anbar 31001, Iraq. [2]Department of Chemical Engineering, Faculty of Engineering, Islamic University of Madinah, Madinah, Saudi Arabia. [3]Sustainability Research Center, Islamic University of Madinah, Madinah, Saudi Arabia. [4]Department of Medical Analysis, Medical Laboratory Technique College, the Islamic University, Najaf, Iraq. [5]Department of Chemistry and Biochemistry, School of Sciences, JAIN (Deemed to be University), Bangalore, Karnataka, India. [6]University Institute of Pharma Sciences, Chandigarh University, Mohali, Punjab, India. [7]Department of Chemistry, Sathyabama Institute of Science and Technology, Chennai, Tamil Nadu, India. [8]Department of Forensic Medicine & Toxicology, IMS and SUM Hospital, Siksha 'O' Anusandhan (Deemed to be University), Bhubaneswar 751003, Odisha, India. [9]Department of Medical Laboratories Technology, Al-nisour University College, Nisour Seq. Karkh, Baghdad, Iraq. [10]Department of Pharmaceutical Chemistry, College of Pharmacy, University of Mosul, Mosul 41001, Iraq. [11]Sharda School of Engineering and Sciences, Sharda University, Greater Noida, UP, India. ✉email: ammar.yasir@uoa.edu.iq; hamad.almohamadi@outlook.com; hha@iu.edu.sa

then various other functional groups on the aromatic ring, or even be completely removed via reactions like the Sandmeyer reaction[12,13]. This versatility has led many chemists to focus on nitroarene reduction as a powerful synthetic tool.

Despite significant advancements in the catalytic reduction of nitroarenes, established methodologies frequently utilize noble or expensive transition metals, including $LiAlH_4$, Fe, Sn, Ag, Co, Pd, Pt, Ru, Rh, Ir, and Ni[11,14–25]. Among these, palladium is often considered a superior catalyst for this transformation due to its high activity and selectivity, albeit at a considerable cost[15,24,26]. These protocols are often characterized by inherent limitations such as the requirement for hazardous ligands and solvents, elevated reaction temperatures, and the use of high-pressure hydrogen[6,24,27,28]. Moreover, the prevalence of homogeneous catalysis in these approaches typically results in intricate and costly separation procedures, further contributing to their overall economic and environmental burden.

In recent years, the adoption of heterogeneous catalysts has emerged as a promising solution to overcome the limitations associated with homogeneous systems[29]. Among various solid supports which were used by organic chemists, magnetic nanoparticles, particularly Fe_3O_4, have proven exceptionally advantageous[30–35]. Their nanoscale dimensions and innovative magnetic separation capabilities simplify both functionalization procedures and catalyst recycling from reaction mixtures[32,36–38]. These magnetic nanoparticles can effectively immobilize transition metal complexes as heterostructures, significantly reducing overall costs by enabling repeated catalyst use[34,39,40].

To address the aforementioned challenges, our current study focuses on synthesizing a novel palladium complex immobilized on the surface of Fe_3O_4 nanoparticles. This heterogeneous nanomagnetic catalyst aims to facilitate the efficient reduction of toxic nitroarenes into their corresponding, highly valuable aniline derivatives. The main novelty of our work lies in the utilization of 2-picolylamine as a ligand for palladium complexation, which plays a crucial role in the room temperature reduction of nitroarenes under green conditions. This system demonstrates excellent catalytic activity across a broad scope of substrates, including aryl and heteroaryl arenes. While previous studies have reported supported palladium catalysts for nitroarene reduction, these systems often face challenges such as difficult separations (requiring filtration)[26], the use of expensive metals such as Au as co-catalysts in bimetallic systems[26], higher reaction temperatures[41], and limited reaction scope[15]. In contrast, our approach offers a magnetically separable palladium catalyst, enabling mild reaction conditions and high substrate versatility, overcoming these common limitations and providing a more efficient and sustainable solution for nitroarene reduction.

Experimental

Materials and methods

All of the chemicals and solvents were acquired from Merck Millipore and Sigma-Aldrich companies and used without further purification. The progress of the reactions was monitored by thin-layer chromatography (TLC) using silica gel 60 F_{254} aluminum-backed plates (Merck Millipore, Germany; catalog no. 1.05554). FTIR spectra were recorded using a Thermo AVATAR spectrometer (USA) with KBr pellets for sample preparation. The crystalline structure of the samples was analyzed using an X-ray diffractometer (PHILIPS PW1730, Netherlands) operating with Cu Kα radiation (λ = 1.54056 Å) at 40 kV and 30 mA, with a step size of 0.05° and a counting time of 1 s per step. Thermal analysis (TGA) was performed using a TA Instruments Q600 (USA) system under Air gas atmospheres. The elemental composition and surface mapping of the samples were characterized using a TESCAN VEGA 3 scanning electron microscope (Czech Republic) equipped with a SAMX EDX detector (France). The elemental concentration of the palladium was further determined by inductively coupled plasma–optical emission spectroscopy (ICP-OES) using a Perkin-Elmer 5300 DV instrument (USA). Surface morphology was examined using TESCAN SEM and FESEM instruments (models VEGA 3, MIRA II, and MIRA III, Czech Republic) to obtain both low- and high-resolution images. The microstructure of the samples was further investigated by transmission electron microscopy (TEM) using a CM120 instrument (Netherlands) operated at an accelerating voltage of 100 kV. Magnetic properties were measured using a vibrating sample magnetometer (VSM, MDKB, Magnatis Kavir Kashan, Iran) with a maximum applied magnetic field of 2 T in a 10 mm air gap, a dynamic range of 500–0.00005 emu at 10 points/s, a noise level of 0.00005 emu, and field resolutions of 2 Oe (low field) and 1 Oe (high field) at room temperature.

Typical procedure for synthesis of [Fe_3O_4@PTMS-2-picolylamine-$PdCl_2$] nanocomposite

The Fe_3O_4 MNPs were synthesized via a co-precipitation method using iron (II) chloride tetrahydrate and iron (III) chloride hexahydrate ($FeCl_2$:$FeCl_3$ molar ratio of approximately 1:2) as precursors, and 25% ammonium hydroxide as the precipitating agent as previously reported in literature[42]. Then 8 g of Fe_3O_4 MNPs were dispersed in 250 mL of toluene for 1 h before the rapid addition of (3-Chloropropyl)trimethoxysilane (CPTMS) (75 mmol, 16.38 g). The reaction mixture was then vigorously stirred at maximum speed at 80 °C for 48 h, during which the surface of Fe_3O_4 MNPs was coated by the silanization agent. The resulting Fe_3O_4@CPTMS composite was isolated using an external neodymium magnet, washed multiple times with *n*-hexanes to remove unreacted CPTMS and other impurities, and then dried in an oven at 80 °C for 4 h. Subsequently, a mixture of 2-picolylamine (12.5 mmol, 1.351 g) and anhydrous K_2CO_3 (7 mmol, 0.967 g) was added to a well-dispersed suspension of Fe_3O_4@CPTMS in DMF (5 g in 150 mL). The reaction mixture was vigorously stirred under reflux conditions for 48 h to facilitate the grafting of 2-picolylamine. The obtained Fe_3O_4@PTMS-2-picolylamine product was separated using an external neodymium magnet, washed thoroughly multiple times with ethanol and water, and dried in an oven at 80 °C for 4 h.

Finally, 2 g of Fe_3O_4@PTMS-2-picolylamine MNPs were added to 100 mL of 95% ethanol and sonicated for 1 h. To this suspension, 4 mmol of $PdCl_2$ was added, and the reaction mixture was stirred under reflux conditions for 24 h. Following this, the reaction was cooled to room temperature, and 3 equivalents of $NaBH_4$ were added.

The refluxing was continued for 8 h to ensure complete reduction of Pd(II) to Pd(0) and its incorporation into the composite. The final [Fe_3O_4@PTMS-2-picolylamine-$PdCl_2$] nanocomposite was isolated using an external magnetic field, washed extensively with hot water and ethanol to remove any unreacted reagents and soluble by-products, and then dried at 80 °C for 4 h (Fig. 1).

General procedure for reduction of nitroarenes over the catalysis of [Fe_3O_4@PTMS-2-picolylamine-$PdCl_2$] nanocomposite

A mixture of nitroarene (1.0 mmol), sodium borohydride (5.0 mmol), and [Fe_3O_4@PTMS-2-picolylamine-$PdCl_2$] (5 mg, 0.2 mol%) were combined in a round-bottom flask with 5 mL of deionized water. The reaction mixture was vigorously stirred at room temperature for 25–90 min and its progress monitored by thin-layer chromatography (TLC) until completion. Afterwards, the catalyst was efficiently separated using an external magnet. The resulting crude product was then extracted with ethyl acetate (3 × 15 mL). The combined organic layers were dried over anhydrous sodium sulfate (Na_2SO_4), and the solvent was removed under reduced pressure using a rotary evaporator. Finally, the residue was purified by column chromatography using a *n*-hexanes/ethyl acetate system as the eluent to provide corresponding pure products in 81–98% yields.

Results and discussions

In this study, a novel palladium catalyst was successfully immobilized on the surface of magnetic nanoparticles through a concise three-step procedure. This involved the initial surface functionalization of Fe_3O_4 with (3-chloropropyl)trimethoxysilane (CPTMS), serving as the C-Cl source. Subsequently, the chloro-groups were substituted with 2-picolylamine, followed by final complexation with $PdCl_2$ to yield the desired nanomagnetized palladium catalytic sites (Fig. 1). The resulting catalyst was thoroughly characterized using various physicochemical analyses to ascertain its precise chemical composition, structural properties, and morphology.

Catalyst characterizations

The Fourier-transform infrared (FT-IR) spectra of Fe_3O_4, Fe_3O_4@CPTMS and [Fe_3O_4@PTMS-2-picolylamine-$PdCl_2$] nanocomposite are shown in Fig. 2. In all spectra, the absorption peaks at 3445 and 625–565 cm^{-1} are attributed to the stretching vibrations of the O–H and Fe–O bands[43]. In the FT-IR spectra of Fe_3O_4@CPTMS and [Fe_3O_4@PTMS-2-picolylamine-$PdCl_2$] nanocomposite, the aliphatic C–H and Si–O stretching bands appear at 2923, 1039, and 1117 cm^{-1}, respectively[43]. In the [Fe_3O_4@PTMS-2-picolylamine-$PdCl_2$] nanocomposite, the aromatic C–H vibrations of the pyridine ring appear at 3048 cm^{-1}, and the introduction of picolylamine metal complex onto the magnetite surface is confirmed by the presence of distinct C = N and C = C stretching peaks at 1671, 1642, and 1597 cm^{-1}, respectively[44].

The crystalline structure of the [Fe_3O_4@PTMS-2-picolylamine-$PdCl_2$] nanocomposite was analyzed by XRD (Fig. 3). The diffractogram prominently displays seven characteristic peaks at 2θ values of 29.93°, 35.43°, 43.18°, 53.18°, 56.98°, and 62.58°. These correspond to the (220), (311), (400), (422), (511) and (440) and planes of the inverse spinel structure of Fe_3O_4 (JCPDS Card No. 01–075-0449)[45]. The presence and intensity of these peaks confirm the high crystallinity of the Fe_3O_4 core and indicate that its crystalline phase remained stable during functionalization. A distinct peak observed at 2θ = 39.83° is attributed to the (111) plane of metallic palladium

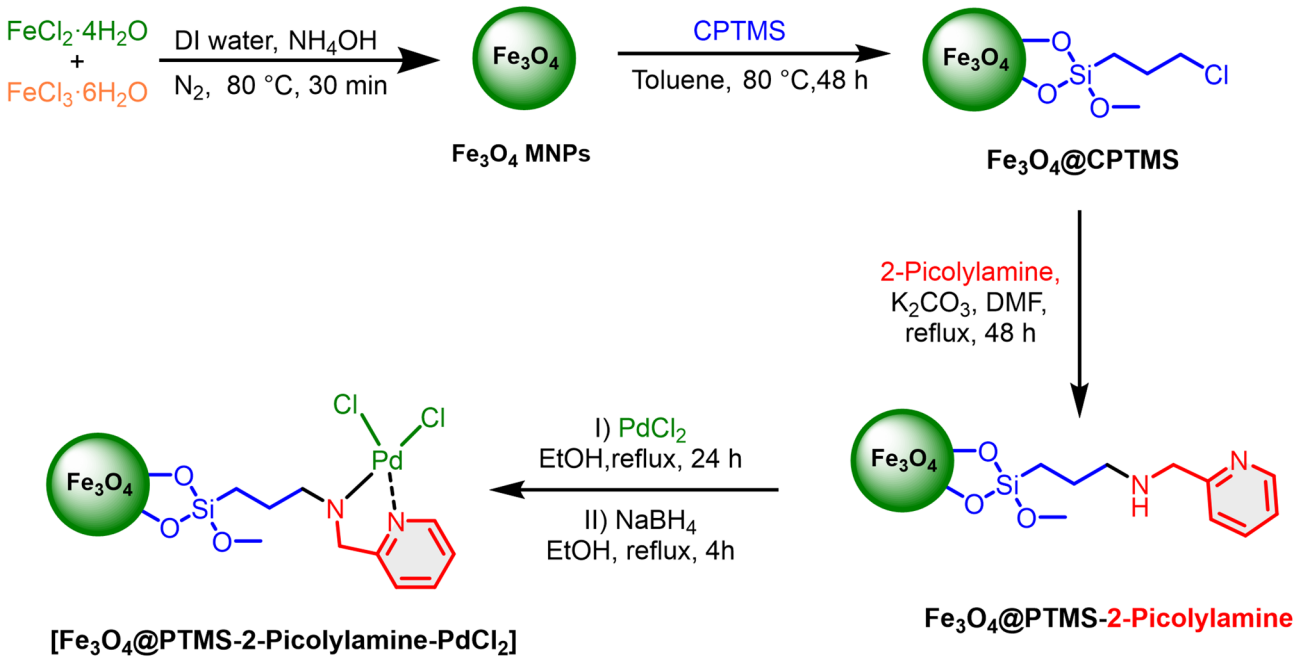

Fig. 1. Stepwise synthesis of [Fe_3O_4@PTMS-2-picolylamine-$PdCl_2$] nanocomposite.

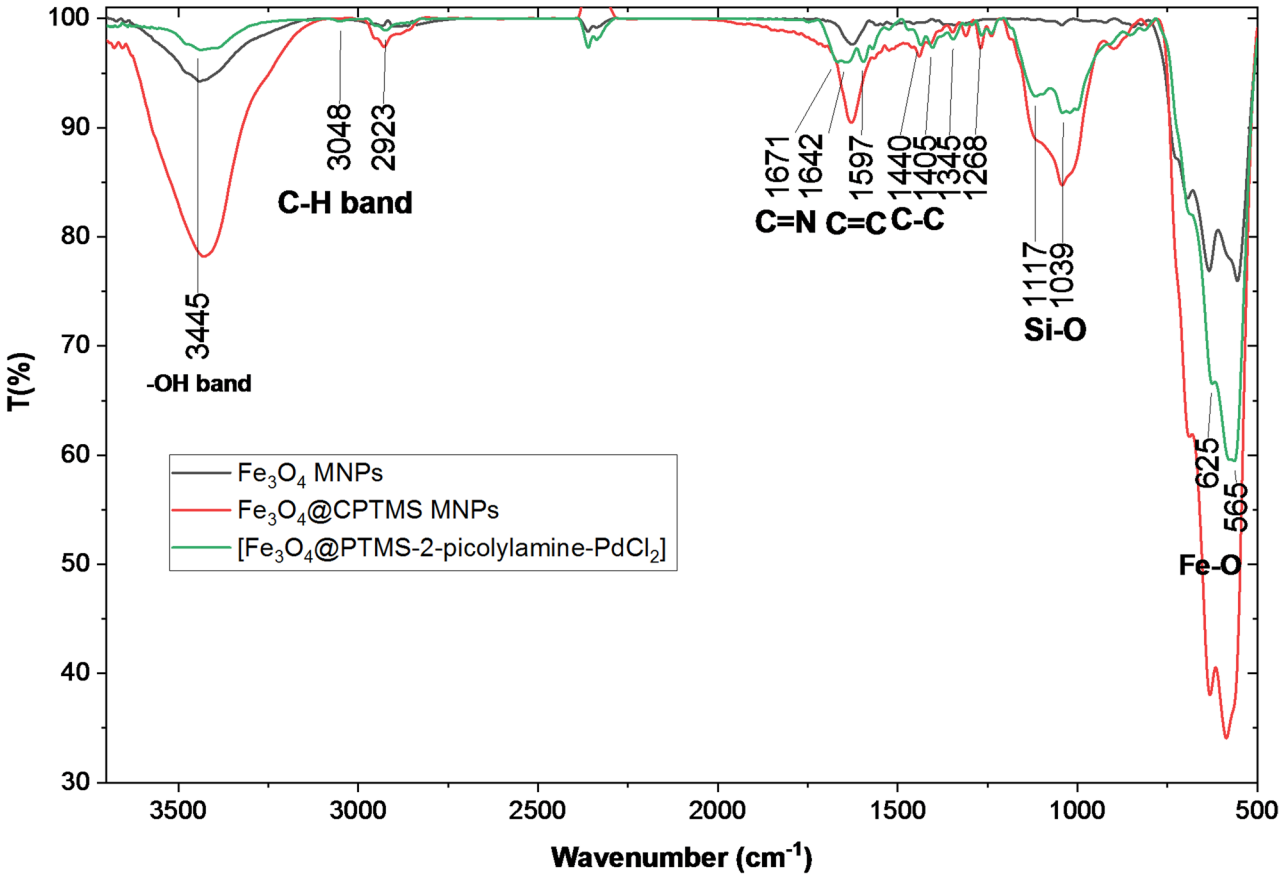

Fig. 2. FT-IR spectra of Fe_3O_4, Fe_3O_4@CPTMS and [Fe_3O_4@PTMS-2-picolylamine-$PdCl_2$] nanocomposite.

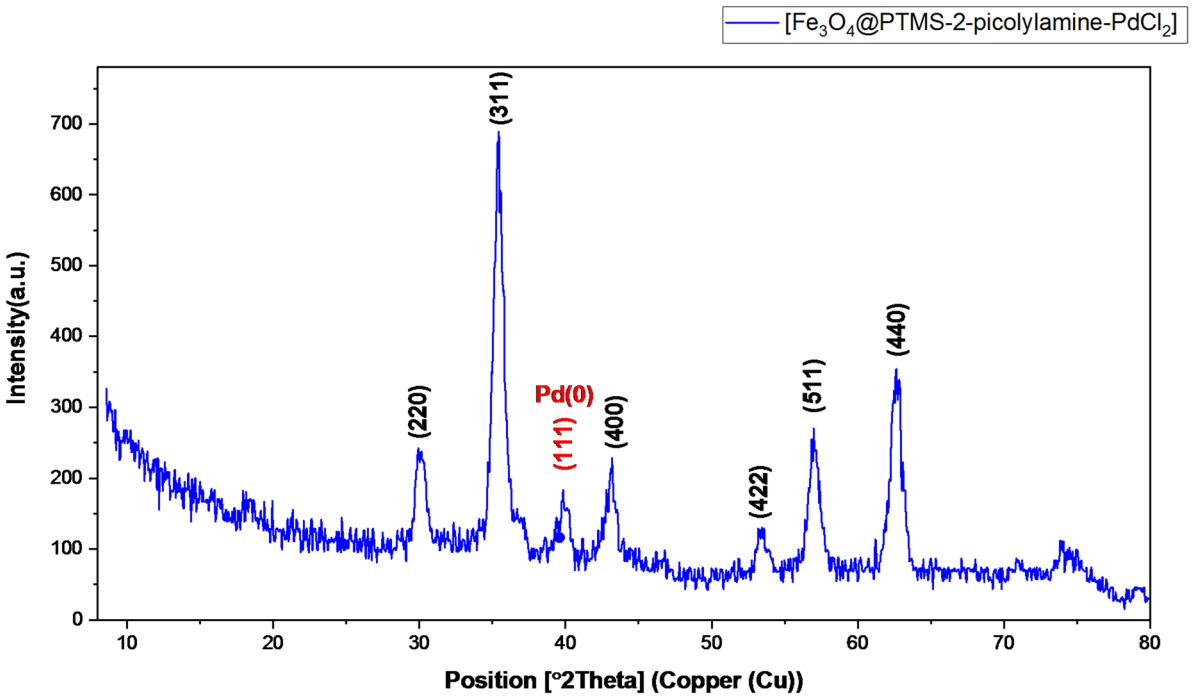

Fig. 3. XRD pattern of [Fe_3O_4@PTMS-2-picolylamine-$PdCl_2$] nanocomposite.

(Pd(0)) (JCPDS Card No. 46–1043)[46]. This confirms the successful immobilization of Pd(0) complex onto the nanocomposite surface, validating the synthesis of the targeted catalyst. Moreover, XRD analysis revealed the crystalline nature of the catalyst, with an average particle size of ~ 18 nm as calculated using the Debye–Scherrer equation.

Thermogravimetric analysis (TGA) (Fig. 4) was employed to assess the thermal stability and quantify the organic and inorganic components of the synthesized [Fe_3O_4@PTMS-2-picolylamine-$PdCl_2$] nanocomposite. An initial weight loss of approximately 1.5% was observed below 200 °C, attributed to the desorption of surface-adsorbed moisture and residual solvent. Subsequently, a significant weight loss of about 8.85% occurred between 200 °C and 600 °C. This major decomposition step confirms the successful functionalization of the particles with the [PTMS-2-picolylamine-$PdCl_2$] complex, as it corresponds to the thermal degradation of the organic material. These findings indicate that the catalyst exhibits thermal stability exceeding 200 °C, making it suitable for applications at elevated temperatures.

The elemental composition of the [Fe_3O_4@PTMS-2-picolylamine-$PdCl_2$] nanocomposite was investigated using EDX analysis, as presented in Fig. 5. The primary matrix elements were identified as iron (58.59 wt%, 30.13 at%) and oxygen (27.03 wt%, 48.53 at%), consistent with the Fe_3O_4 catalyst support. The successful immobilization of CPTMS was corroborated by the detection of silicon (1.67 wt%, 1.70 at%). Furthermore, the presence of carbon (6.60 wt%, 15.78 at%) and nitrogen (0.92 wt%, 1.90 at%) confirmed the successful grafting of both CPTMS and 2-picolylamine onto the nanocomposite. Finally, the detection of palladium (4.17 wt%, 1.13 at%) and chlorine (1.03 wt%, 0.83 at%) unequivocally verified the successful immobilization of palladium dichloride and the formation of the desired complex. To quantitatively validate the palladium loading, ICP-OES analysis determined the Pd content to be 3.97×10^{-4} mol/g, which is in excellent agreement with the EDX data.

The elemental distribution across the catalyst surface was meticulously examined using WDX analysis, as depicted in Fig. 6. The resulting elemental maps provide crucial insights into the spatial arrangement of each component. As expected, iron and oxygen exhibit a high density and widespread distribution, forming the foundational matrix of the catalyst. Silicon and carbon show a relatively lower, yet still significant, dispersion across the surface, confirming their successful incorporation. Nitrogen is present with a lower overall density and a more localized dispersion, consistent with the specific grafting of the 2-picolylamine. Crucially, palladium and chlorine display a remarkably uniform distribution across the entire catalyst surface, and have a similar distribution pattern. The excellent dispersion of palladium is particularly noteworthy, as it suggests high accessibility for reactants during catalytic applications, a key factor for optimal catalytic performance. This uniform distribution bodes well for the catalyst's efficiency and activity.

Scanning electron microscopy (SEM) images of the [Fe_3O_4@PTMS-2-picolylamine-$PdCl_2$] nanocomposite are displayed in Fig. 7. The material consistently exhibits a uniform nanoscale spherical morphology. Quantitative analysis revealed that the primary nanoparticles possess diameters predominantly within the 40–90 nm range. However, a significant tendency for these individual nanoparticles to aggregate was observed, leading to the formation of larger, rough, quasi-spherical clusters, potentially as a consequence of the multi-step surface functionalization.

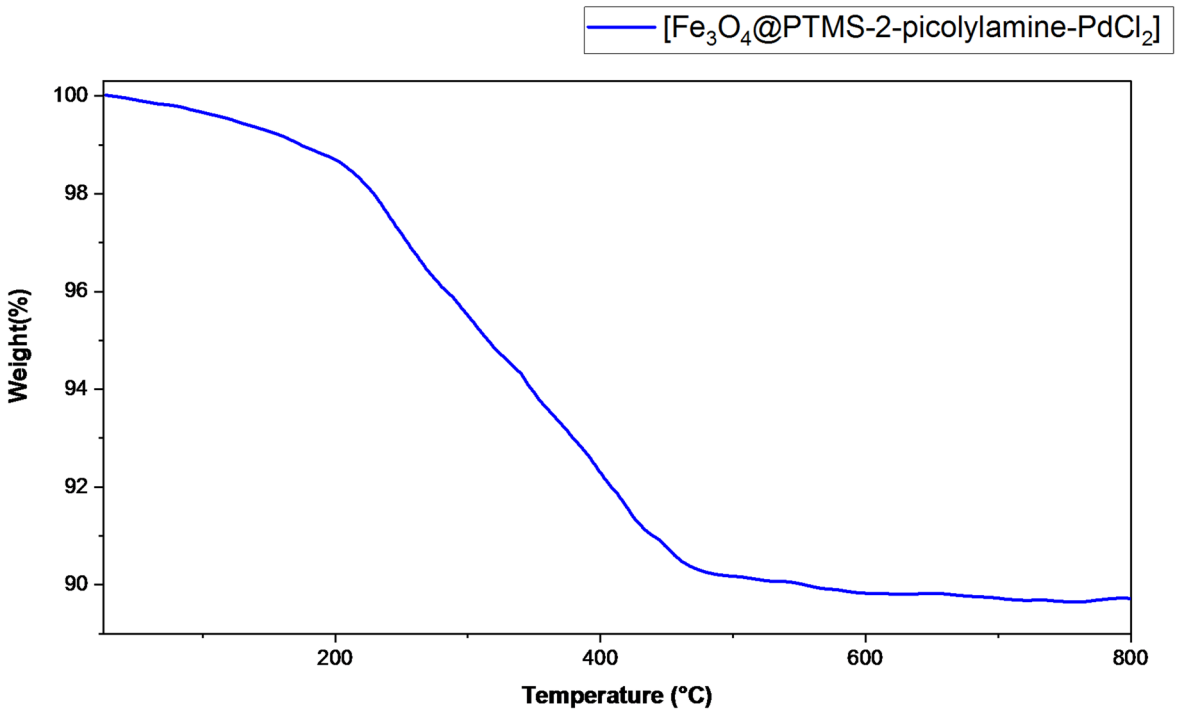

Fig. 4. TGA analysis of [Fe_3O_4@PTMS-2-picolylamine-$PdCl_2$] nanocomposite.

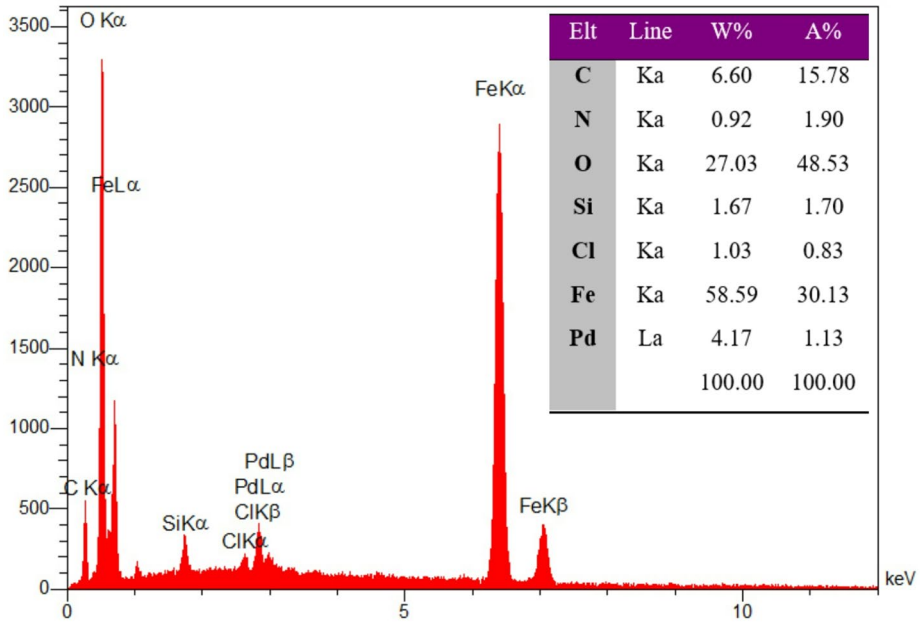

Elt	Line	W%	A%
C	Ka	6.60	15.78
N	Ka	0.92	1.90
O	Ka	27.03	48.53
Si	Ka	1.67	1.70
Cl	Ka	1.03	0.83
Fe	Ka	58.59	30.13
Pd	La	4.17	1.13
		100.00	100.00

Fig. 5. EDX analysis of [Fe_3O_4@PTMS-2-picolylamine-$PdCl_2$] nanocomposite.

TEM analysis was employed to characterize the morphology, particle size, and distribution of the [Fe_3O_4@PTMS-2-picolylamine-$PdCl_2$] nanocomposite. As depicted in Fig. 8, the micrograph clearly reveals nanostructured particles exhibiting a predominantly spherical or quasi-spherical morphology. The high electron density of the dark core unequivocally confirms the presence of Fe_3O_4 nanoparticles, while the surrounding lighter layer is attributed to the successful surface functionalization with the [PTMS-2-picolylamine-$PdCl_2$] moiety. The analysis demonstrates an average particle size in the range of 5–20 nm, consistent with the XRD data, and highlights a marked propensity for aggregation, resulting in larger clustered domains embedded within a lighter matrix. These comprehensive TEM observations collectively corroborate the successful synthesis and formation of the targeted [Fe_3O_4@PTMS-2-picolylamine-$PdCl_2$] nanocomposite.

The magnetic behavior of the [Fe_3O_4@PTMS-2-picolylamine-$PdCl_2$] nanocomposite was examined using Vibrating Sample Magnetometry (VSM), and the corresponding hysteresis curve is shown in Fig. 9. The nanocomposite exhibits a saturation magnetization (Ms) of 22.17 emu g^{-1}, which is lower than that of bare Fe_3O_4. This decrease confirms the successful deposition of non-magnetic organic (CPTMS and 2-picolylamine, and palladium) layers on the magnetic core. Despite the reduction in Ms, the nanocomposite preserves sufficient magnetic responsiveness for rapid collection using an external neodymium magnet, ensuring its effective recyclability in catalytic applications. Importantly, the hysteresis loop displays negligible remanence and very low coercivity (Hc), characteristic features of superparamagnetic nanoparticles. The near-zero coercive field indicates that the magnetic moments can rapidly randomize in the absence of an external field, while the S-shaped curve without noticeable magnetic hysteresis confirms the absence of long-range ferromagnetic ordering. This behavior is expected for Fe_3O_4 nanoparticles with sizes below the single-domain limit, even after surface modification.

Catalytic study

The catalytic performance of the synthesized [Fe_3O_4@PTMS-2-picolylamine-$PdCl_2$] nanocomposite was comprehensively evaluated for the reduction of nitroarenes to their corresponding anilines. The reduction of nitrobenzene using sodium borohydride served as the model reaction, allowing for a systematic optimization of critical reaction parameters including catalyst type, catalyst loading, solvent, and reducing agent concentration (Table 1). Control experiments rigorously confirmed that neither catalyst-free systems nor individual catalyst precursors demonstrated any activity, unequivocally establishing that the Pd complex on [Fe_3O_4@PTMS-2-picolylamine-$PdCl_2$] nanocomposite is solely responsible for initiating and driving the reaction. Optimization of catalyst loading showed a direct correlation between catalyst amount and product yield. A maximum yield of 85% was achieved with 5 mg of the catalyst; however, increasing the loading to 6 mg offered no further enhancement. Solvent screening revealed distinct influences on reaction efficiency. While both DMF and PEG-400 improved yields, they concurrently prolonged reaction times. Remarkably, water emerged as the optimal solvent, facilitating a 98% yield in just 15 min. Probably, enhanced performance in water arises from, improved hydrophilicity of the catalyst surface, increased solubility and dispersion of $NaBH_4$, and more efficient mass transfer of reactive hydride species compared with organic media. These factors collectively promote faster electron transfer and more effective generation of Pd–H intermediates, which ultimately improves the reduction efficiency of nitroarenes in aqueous conditions. This exceptional performance led to its selection as the ideal reaction medium. Finally, the concentration of the reducing agent was optimized. Decreasing the $NaBH_4$

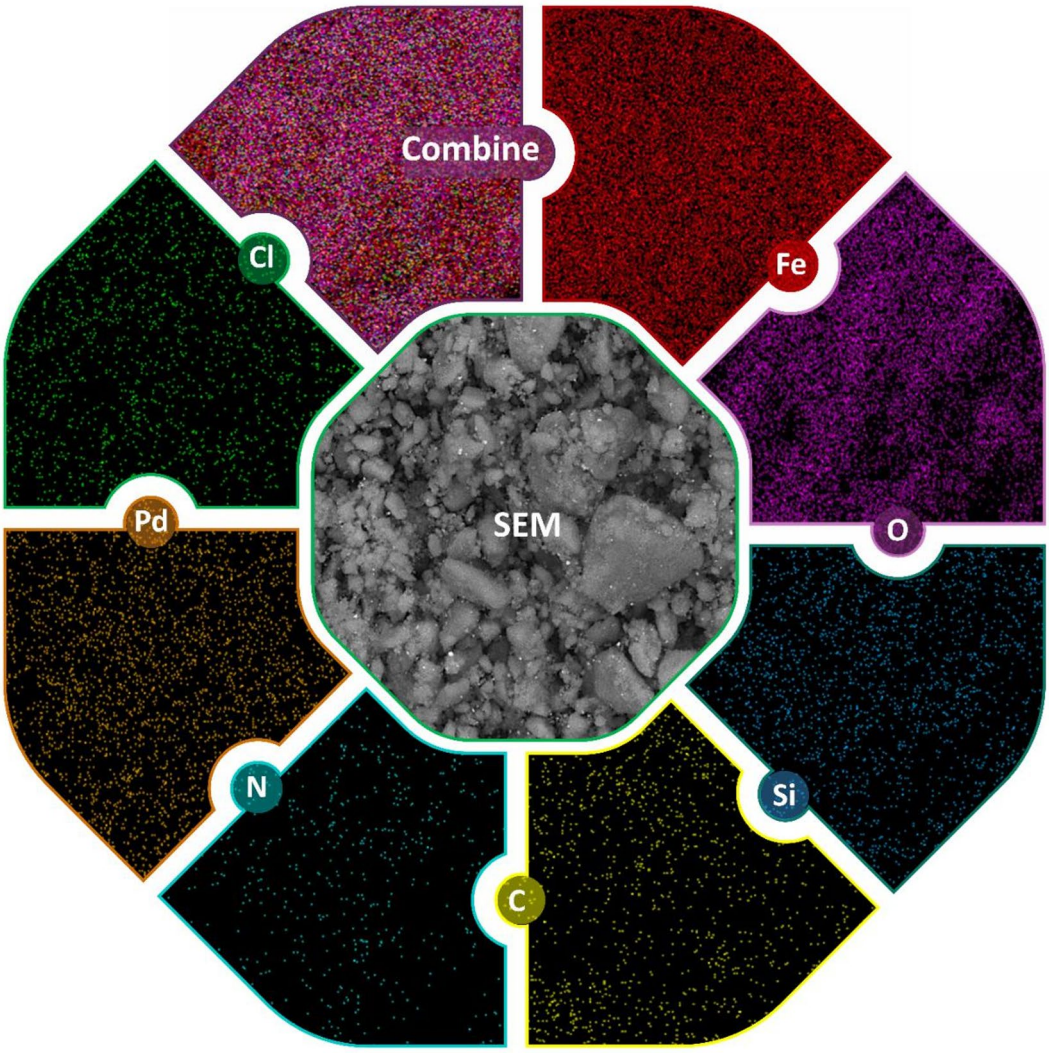

Fig. 6. Elemental mapping analysis of [Fe_3O_4@PTMS-2-picolylamine-$PdCl_2$] nanocomposite.

amount from 5 mmol to 3 or 2 mmol adversely affected both reaction time and yield. Consequently, 5 mmol of $NaBH_4$ was determined to be the optimal concentration for achieving high efficiency and rapid conversion. Finally, the optimal conditions for the nitrobenzene reduction were determined to be 5 mg of [Fe_3O_4@PTMS-2-picolylamine-$PdCl_2$] nanocomposite (corresponding to 0.2 mol% Pd), 5 mmol of $NaBH_4$, and water as the solvent at room temperature.

In the next step, With the optimized reaction conditions established, the scope and applicability of the methodology were thoroughly investigated using a diverse range of nitroarenes bearing various substituents, including both electron-donating and electron-withdrawing groups on the aryl ring (Table 2). The findings revealed a clear influence of electronic properties on reactivity. Nitro compounds substituted with electron-donating groups exhibited enhanced reactivity, leading to higher yields in shorter reaction times, compared to those with electron-withdrawing groups. Conversely, steric hindrance was observed to decrease reactivity. When dinitro compounds were employed, a notable increase in reaction time was observed, accompanied by a decrease in the corresponding yield, with the final product consistently identified as the diamine. Overall, the developed method demonstrated excellent functional group tolerance and broad applicability across a wide spectrum of nitroarene substrates.

Reaction mechanism

A plausible Pd-mediated hydride-transfer mechanism for reduction of nitroarenes over the catalysis of [Fe_3O_4@PTMS-2-picolylamine-$PdCl_2$] nanocomposite which is consistent with prior studies is outlined in Fig. 10[57,58]. Initially the $NaBH_4$ reacts with water and generated hydrogen that was rapidly adsorbed onto the surface of the catalyst. This adsorption promotes efficient electron delivery to the palladium centers, enabling the generation of catalytically active Pd–H species through dehydrogenation of BH_4^-. The strong metal–hydride character of these intermediates has been widely recognized as the key driving force in borohydride-based hydrogenation systems. The nitroarene substrate subsequently approaches the metal surface and coordinates through the electrophilic

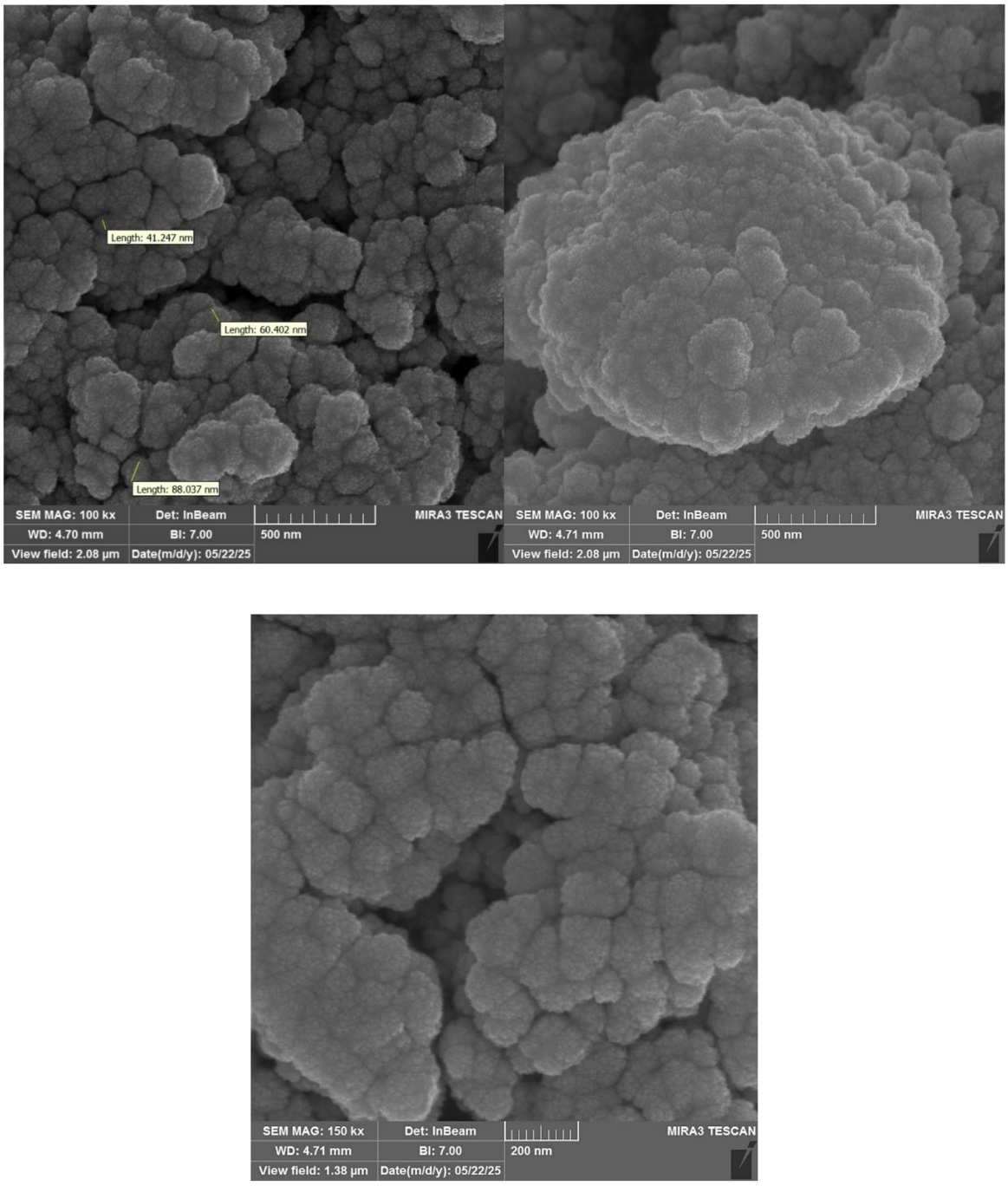

Fig. 7. SEM images of [Fe_3O_4@PTMS-2-picolylamine-$PdCl_2$] nanocomposite.

$-NO_2$ group. The activated Pd–H species then undergo hydrogen bonding to nitrogen center, initiating a stepwise hydrogenation sequence. This sequence typically involves the formation of nitroso and hydroxylamine intermediates; each stabilized transiently on the palladium surface. Successive hydride and proton transfers ultimately furnish the corresponding aniline derivative.

Reusability, hot filtration and leaching tests

A primary objective of this study was to develop a heterogeneous and recyclable catalyst. To evaluate these crucial parameters, reusability, hot filtration, and leaching tests were conducted. The reduction of nitrobenzene under optimal conditions served as the model reaction for these investigations. After the initial reaction, the catalyst was efficiently separated using an external magnet, washed with ethyl acetate and water, and then dried at 80 °C for 4 h. It was then reintroduced into the next reaction cycle using fresh nitrobenzene and $NaBH_4$. This process was repeated for five consecutive cycles. The results demonstrate that the catalyst could be recovered and utilized for five cycles without any noticeable decrease in activity, confirming its excellent reusability (Fig. 11).

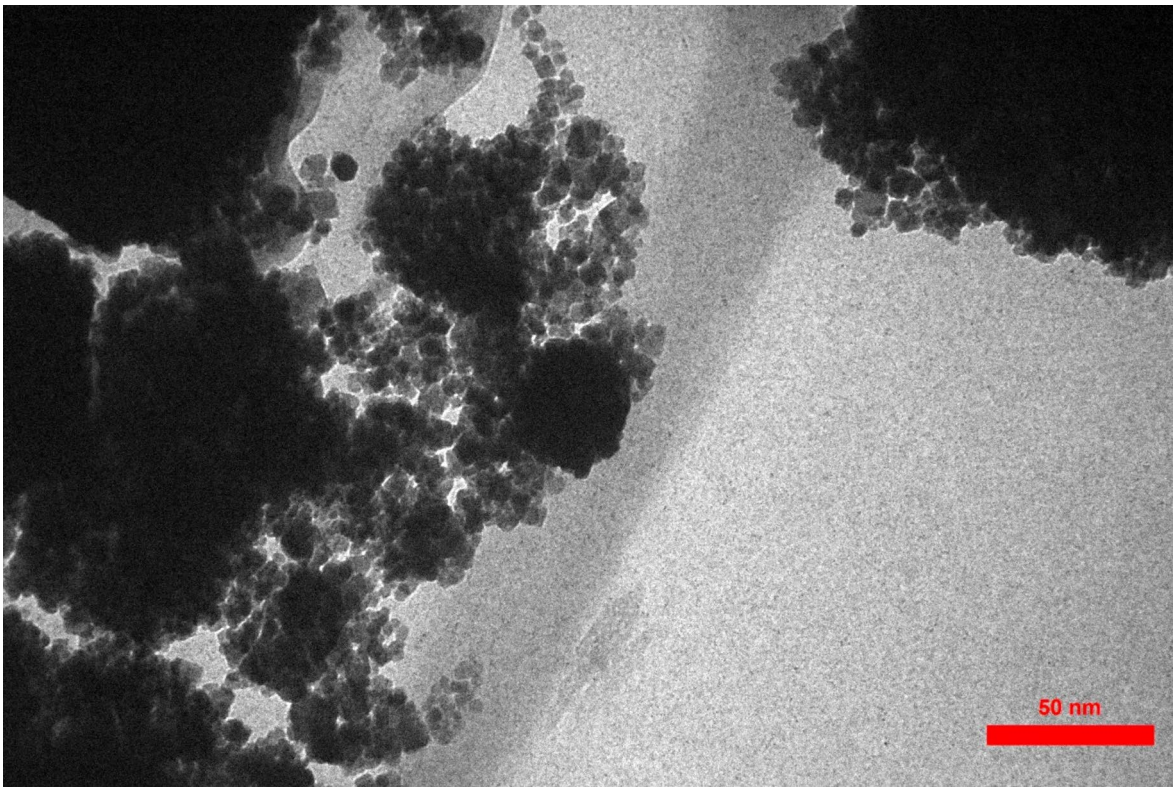

Fig. 8. TEM images of [Fe_3O_4@PTMS-2-picolylamine-$PdCl_2$] nanocomposite.

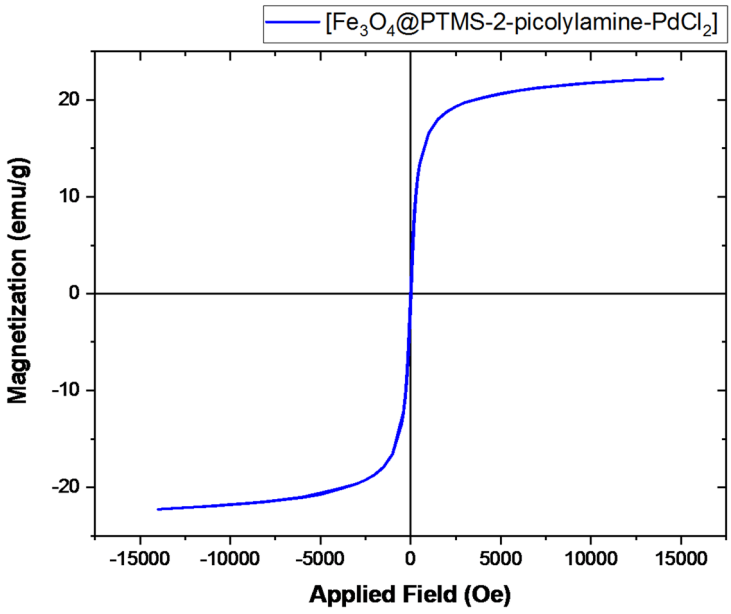

Fig. 9. VSM analysis of [Fe_3O_4@PTMS-2-picolylamine-$PdCl_2$] nanocomposite.

The structural integrity of the recovered [Fe_3O_4@PTMS-2-picolylamine-$PdCl_2$] catalyst was verified through SEM analysis, which confirmed its morphological stability and unambiguously validated its robustness under operational conditions (Fig. 12).

To further confirm the heterogeneous nature of the catalyst, a hot filtration test was performed using the same model reaction. After 5 min of reaction, the catalyst was separated, yielding 69% of the desired product. The filtrate was then allowed to continue reacting under optimal conditions, but only an additional 2% conversion was observed. This minimal progress strongly indicates the heterogeneous nature of the catalyst in the reaction

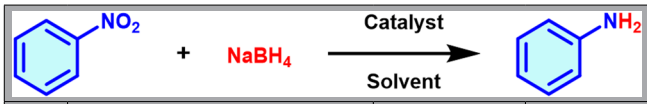

Entry	Catalyst	Catalyst Amount (mg)	$NaBH_4$amount (mmol)	Solvent	Time (min)	Yield (%)[a, b]
1	-	-	5	Ethanol	120	Trace
2	Fe_3O_4	5	5	Ethanol	240	Trace
3	Fe_3O_4@CPTMS	5	5	Ethanol	240	Trace
4	Fe_3O_4@PTMS-2-picolylamine	5	5	Ethanol	240	Trace
5	[Fe_3O_4@PTMS-2-picolylamine-$PdCl_2$]	2	5	Ethanol	30	45
6	[Fe_3O_4@PTMS-2-picolylamine-$PdCl_2$]	4	5	Ethanol	30	77
7	[Fe_3O_4@PTMS-2-picolylamine-$PdCl_2$]	5	5	Ethanol	30	85
8	[Fe_3O_4@PTMS-2-picolylamine-$PdCl_2$]	6	5	Ethanol	30	85
9	[Fe_3O_4@PTMS-2-picolylamine-$PdCl_2$]	5	5	DMF	95	87
10	[Fe_3O_4@PTMS-2-picolylamine-$PdCl_2$]	5	5	PEG-400	55	91
11	[Fe_3O_4@PTMS-2-picolylamine-$PdCl_2$]	5	5	Water	30	98
12	[Fe_3O_4@PTMS-2-picolylamine-$PdCl_2$]	5	3	Water	45	89
13	[Fe_3O_4@PTMS-2-picolylamine-$PdCl_2$]	5	2	Water	85	71
14	[Fe_3O_4@PTMS-2-picolylamine-$PdCl_2$]	5	-	Water	240	N.R

Table 1. Optimization of nitrobenzene reduction over the catalysis of [Fe_3O_4@PTMS-2-picolylamine-$PdCl_2$] nanocomposite. [a]Isolated yield. [b]Conditions: nitrobenzene (1 mmol), $NaBH_4$ (5 mmol), catalyst (mg) and solvent (5 mL).

medium. Furthermore, to quantitatively support the negligible leaching, ICP–OES measurements were also performed on the recovered catalyst after each cycle. The Pd loadings were 3.87×10^{-4}, 3.81×10^{-4}, 3.72×10^{-4}, 3.64×10^{-4}, and 3.56×10^{-4} mol·g^{-1} for the first through fifth cycles, respectively. This gradual and minor decrease relative to the fresh catalyst confirms the minimal metal leaching during consecutive recycling cycles.

Comparison

The catalytic reduction of nitroarenes is incredibly important in organic synthesis, which is why synthetic chemists have been so interested in it. Many methods have already been developed for this transformation. In this study, we've summarized the latest findings and compared [Fe_3O_4@PTMS-2-picolylamine-$PdCl_2$] catalyst against existing literature (Table 3) to see how well it performs. The comparisons highlight several key advantages of the current catalyst: superior separability via simple magnetic decantation, enhanced reusability, and reduced leaching. Furthermore, the catalyst demonstrates comparable product yields and reaction times, making it an efficient option for aniline synthesis via nitroarene reduction.

Conclusion

In summary, we successfully synthesized a novel, highly dispersed, and exceptionally stable nanomagnetic 2-picolylamine palladium complex supported on Fe_3O_4 nanoparticles, employing a straightforward and efficient method. Comprehensive characterization confirmed the successful immobilization of organic layers on the Fe_3O_4 surface while maintaining the support's crystalline integrity. The resulting catalyst exhibited nanoscale dimensions, excellent thermal stability, high MS value and uniform palladium dispersion. This nanomagnetic palladium complex demonstrated superior catalytic activity for the reduction of nitroarenes to anilines at room temperature in water, a remarkably green solvent. While reaction efficiency was influenced by electronic and steric factors of the nitro group, the catalyst consistently delivered high to excellent yields in short reaction times, surpassing the performance of previously reported systems. Furthermore, extensive reusability tests, including hot filtration and metal leaching analyses, unequivocally established the heterogeneous nature of the catalyst. It maintained its robust catalytic performance and morphology over at least five successive cycles with negligible loss of activity and no significant palladium leaching into the reaction medium. This work presents a highly promising and sustainable catalytic system for nitroarene reduction.

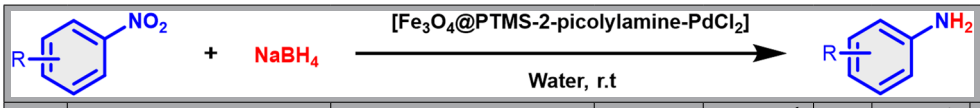

Entry	Nitroarene	Product	Time (min)	Yield (%)[a, b]	TON	TOF (h^{-1})	Melting point (°C)
1	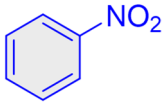	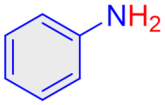	30	98	490	980	Oil[47]
2	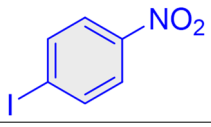	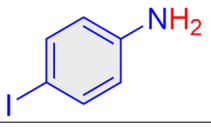	45	95	475	633	62–63[48]
3	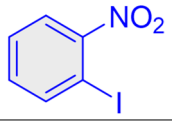	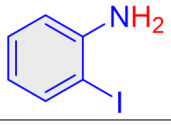	55	90	450	490	57–59[49]
4	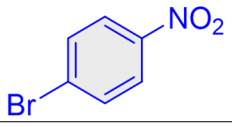	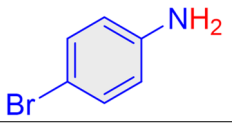	45	95	475	633	59–62[50]
5	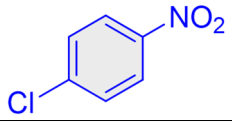	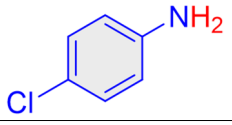	40	97	485	727	73–75[47]
6	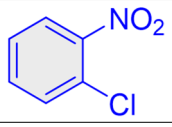	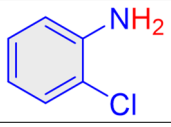	50	95	475	570	Oil[49]
7	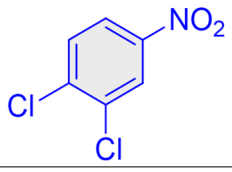	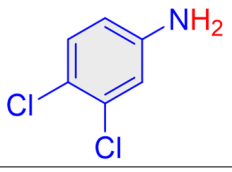	45	97	485	646	59–62[51]
8	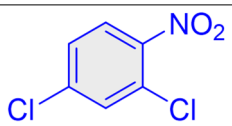	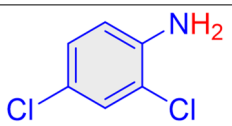	55	94	470	512	26–28[52]
9	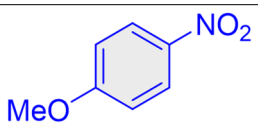	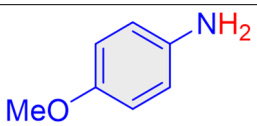	25	98	490	1176	55–57[48]
10	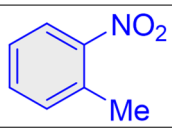	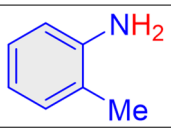	35	91	455	780	Oil[47,49]
11	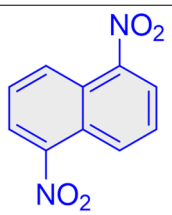	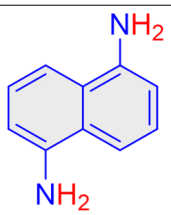	85	88	440	310	185–187[53]
12	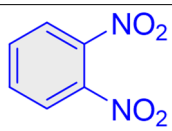	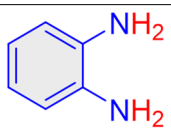	90	81	405	270	103–105[54]

Continued

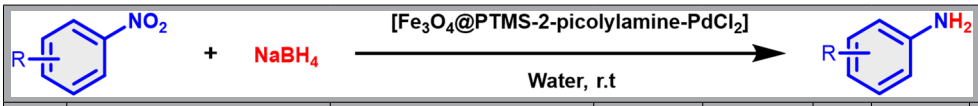

Entry	Nitroarene	Product	Time (min)	Yield (%)[a, b]	TON	TOF (h^{-1})	Melting point (°C)
13	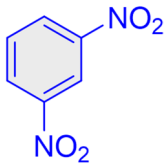	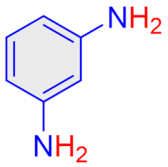	75	83	415	332	62–63[48]
14	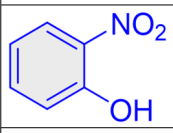	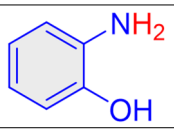	60	88	440	440	118–120[49]
15	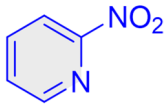	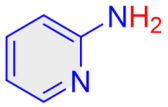	35	96	480	822	59–60[49]
16	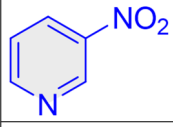	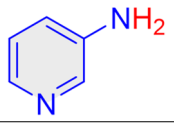	40	94	470	705	64–65[55]
17	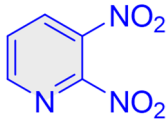	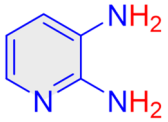	75	84	420	336	114–116[56]

Table 2. The scope of nitroarene reduction over the catalysis of [Fe_3O_4@PTMS-2-picolylamine-$PdCl_2$] nanocomposite. [a]Isolated yield. [b]Conditions: nitroarene (1 mmol), $NaBH_4$ (5 mmol), [Fe_3O_4@PTMS-2-picolylamine-$PdCl_2$] (5 mg, 0.2 mol%) in water (5 mL) at room temperature.

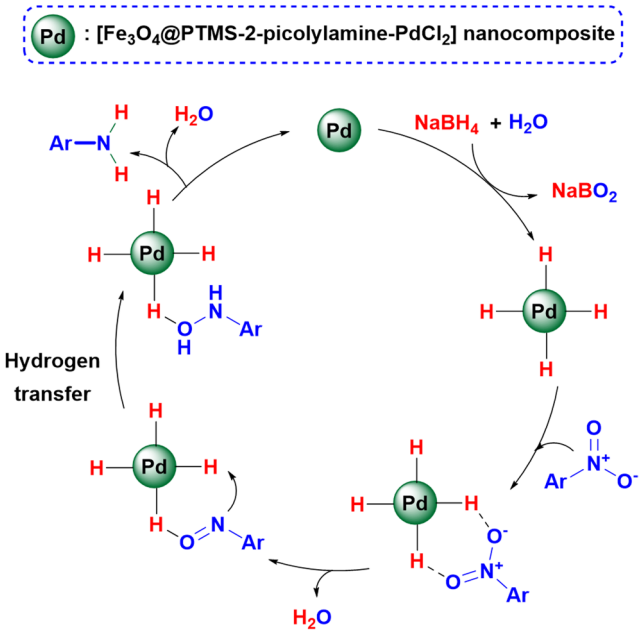

Fig. 10. The plausible mechanism for reduction of nitroarenes over the catalysis of [Fe_3O_4@PTMS-2-picolylamine-$PdCl_2$] nanocomposite.

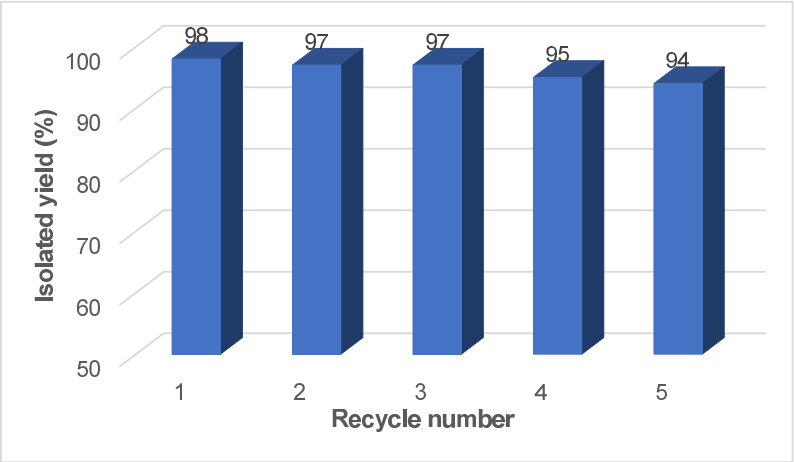

Fig. 11. Reusability of [Fe_3O_4@PTMS-2-picolylamine-$PdCl_2$] in reduction of nitrobenzene.

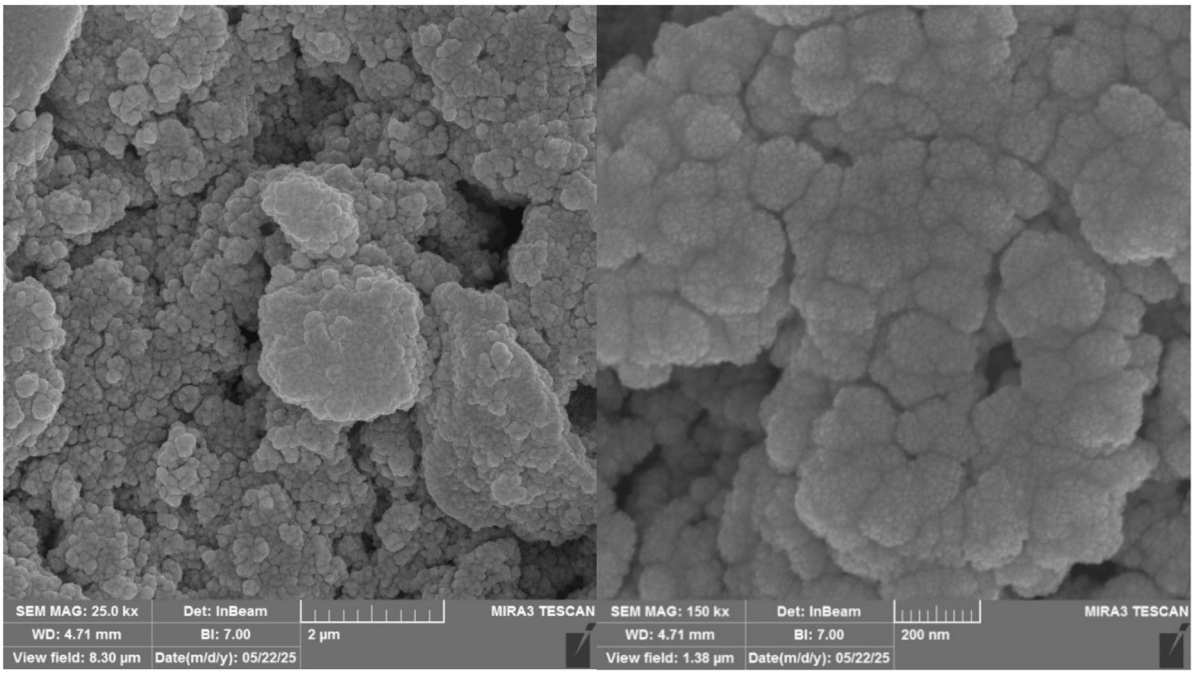

Fig. 12. SEM images of recovered [Fe_3O_4@PTMS-2-picolylamine-$PdCl_2$] catalyst.

Entry	Catalyst	Time	Yield (%) [a]	Reference
1	SPO-Pd-NPs	24 h	96	[59]
2	Fe_3O_4@ β-CD@Pd	1 h	99	[41]
3	Half-Sandwich Ruthenium Complexes	24 h	89	[60]
4	Cu_2O	25 min	92	[28]
5	[Fe_3O_4@PTMS-2-picolylamine-$PdCl_2$]	30 min	98	This work

Table 3. Comparison of [Fe_3O_4@PTMS-2-picolylamine-$PdCl_2$] nanocomposite catalytic efficiency in reduction of nitrobenzene. [a]Isolated yield.

Data availability

Data will be made available on request. Requests for data should be directed to Dr. Hamad AlMohamadi (Email: hamad.almohamadi@outlook.com & hha@iu.edu.sa).

Received: 29 September 2025; Accepted: 1 January 2026
Published online: 07 February 2026

References

1. Patel, S. S., Patel, D. B. & Patel, H. D. Synthetic protocols for aromatic nitration: A review. *ChemistrySelect* **6**, 1337–1356 (2021).
2. Qian, Y. E., Zheng, L., Xiang, H. Y. & Yang, H. Recent progress in the nitration of Arenes and alkenes. *Org. Biomol. Chem.* **19**, 4835–4851 (2021).
3. Biswal, P., Sai Kumar, G. & Chandrasekhar, V. AgSbF 6 catalyzed reduction of nitroarenes by phenylsilane to anilines. *J. Org. Chem.* **90**, 3194–3201 (2025).
4. Asha, K. S., Bhattacharyya, K. & Mandal, S. Discriminative detection of nitro aromatic explosives by a luminescent metal–organic framework. *J. Mater. Chem. C.* **2**, 10073–10081 (2014).
5. Kovacic, P. & Somanathan, R. Nitroaromatic compounds: environmental toxicity, carcinogenicity, mutagenicity, therapy and mechanism. *J. Appl. Toxicol.* **34**, 810–824 (2014).
6. Singh, P., Mukherjee, A., Mahato, A., Pramanik, A. & Dhak, D. A. Review on chemoselective reduction of nitroarenes for wastewater remediation using Biochar supported metal catalysts: kinetic and mechanistic studies. *Chem. Afr.* **6**, 561–578 (2023).
7. Campbell, C. D. & Stewart, M. I. Reflections on the teaching practices for the reduction of nitroarenes: updating methodologies and considerations of the mechanism. *J. Chem. Educ.* **100**, 3171–3178 (2023).
8. Ahmad, H. A. et al. Palladium metal nanoparticles fabricated and stabilized in microgels for reduction of nitrobenzene derivatives. *Inorg. Chem. Commun.* **172**, 113740 (2025).
9. Lakshminarayana, B., Selvaraj, M., Satyanarayana, G. & Subrahmanyam, C. Switching of support materials for the hydrogenation of nitroarenes: A review. *Catal. Rev. - Sci. Eng.* **66**, 259–342 (2024).
10. Gholinejad, M., Elkhani, Z., Nayeri, S. & Sansano, J. M. Nitrogen-enriched carbon nanotube supported palladium as a catalyst for desulfurization of Dibenzothiophene and reduction of nitroarenes. *Sci. Rep.* **15**, 5089 (2025).
11. Asiri, M. et al. Palladium nanoparticles supported on MnFe2O4/SiO2/TT as highly active and reusable catalysts for the reduction of nitroarenes and oxidation of sulfide. *J. Phys. Chem. Solids*. **207**, 112883 (2025).
12. Akhtar, R., Zahoor, A. F., Rasool, N., Ahmad, M. & Ali, K. G. Recent trends in the chemistry of Sandmeyer reaction: a review. *Mol. Divers.* **26**, 1837–1873 (2022).
13. Soleiman-Beigi, M., Mohammadi, M. & Kohzadi, H. An overview on copper in industrial chemistry: from ancient pigment to modern catalysis. *Coord. Chem. Rev.* **529**, 216438 (2025).
14. Kadam, H. K. & Tilve, S. G. Advancement in methodologies for reduction of nitroarenes. *RSC Adv.* **5**, 83391–83407 (2015).
15. Halligudra, G. et al. PdII on Guanidine-Functionalized Fe3O4 nanoparticles as an efficient heterogeneous catalyst for Suzuki–Miyaura Cross-Coupling and reduction of nitroarenes in aqueous media. *ACS Omega*. **6**, 34416–34428 (2021).
16. Liu, Q. et al. Synergy effect of Ru single atoms and clusters on the MoS2 nanosheet for the selective hydrogenation of nitroarenes. *ACS Appl. Nano Mater.* **7**, 22517–22524 (2024).
17. Qiao, J. et al. Magnetically reusable fe3o4@nc@pt catalyst for selective reduction of nitroarenes. *Catalysts* **11**, 1219 (2021).
18. Shukla, A., Singha, R. K., Sasaki, T. & Bal, R. Nanocrystalline Pt-CeO2 as an efficient catalyst for a room temperature selective reduction of nitroarenes. *Green. Chem.* **17**, 785–790 (2015).
19. Chen, S., Lu, G. & Cai, C. Iridium-catalyzed transfer hydrogenation of nitroarenes to anilines. *New. J. Chem.* **39**, 5360–5365 (2015).
20. Li, X. et al. Pt nanoclusters supported on Ti3C2Tx nanosheets for the selective hydrogenation of halogenated nitroarenes under mild conditions. *ACS Appl. Nano Mater.* **7**, 14540–14548 (2024).
21. Yang, Q., Zhang, H. Y., Wang, L., Zhang, Y. & Zhao, J. Ru/UiO-66 catalyst for the reduction of nitroarenes and tandem reaction of alcohol Oxidation/Knoevenagel condensation. *ACS Omega*. **3**, 4199–4212 (2018).
22. Bala, E. et al. Catalytic reduction of nitroarenes under aqueous conditions using magnetically reusable Co3O4 nanoparticles. *Colloids Surf. Physicochem Eng. Asp*. **708**, 135961 (2025).
23. Liu, Z. et al. Crystal facet engineering of Pd/TiO2 to boost the activity and selectivity for nitroarenes hydrogenation. *Chem. Eng. J.* **503**, 158337 (2025).
24. Lu, A. et al. Highly efficient catalytic transfer hydrogenation for the conversion of nitrobenzene to aniline over PdO/TiO2: the key role of in situ switching from PdO to Pd. *J. Environ. Sci.* **148**, 515–528 (2025).
25. Park, M., Rajamanickam, K. R. & Lee, S. Palladium-Catalyzed aminocarbonylation using nitroarenes under NMP-Mediated photochemical conditions. *Org. Lett.* **27**, 6617–6622 (2025).
26. Lakshminarayana, B., Satyanarayana, G. & Subrahmanyam, C. Bimetallic Pd-Au/TiO2 nanoparticles: an efficient and sustainable heterogeneous catalyst for rapid catalytic hydrogen transfer reduction of nitroarenes. *ACS Omega*. **3**, 13065–13072 (2018).
27. Guo, W., Zheng, Y., Xiang, W. & Zhang, Y. Advances in the catalysis of reduction of nitroaromatics and its mechanism: a tutorial review. *RSC Sustain.* **3**, 243–254 (2024).
28. Madasu, M., Hsia, C. F., Rej, S. & Huang, M. H. Cu2O pseudomorphic conversion to Cu crystals for diverse nitroarene reduction. *ACS Sustain. Chem. Eng.* **6**, 11071–11077 (2018).
29. Sedghi, R., Heravi, M., Asadi, M., Nazari, S., Nabid, R. & N. & Recently used nanocatalysts in reduction of nitroarenes. *Curr. Org. Chem.* **20**, 696–734 (2015).
30. Mawlid, O. A., Abdelhady, H. H. & El-Deab, M. S. Recent advances in magnetic Nanoparticle-Based heterogeneous catalysts for efficient biodiesel production: A review. *Energy Fuels*. **38**, 20169–20195 (2024).
31. Zhang, Q., Yang, X. & Guan, J. Applications of magnetic nanomaterials in heterogeneous catalysis. *ACS Appl. Nano Mater.* **2**, 4681–4697 (2019).
32. Polshettiwar, V. et al. Magnetically recoverable nanocatalysts. *Chem. Rev.* **111**, 3036–3075 (2011).
33. Ma, Z., Mohapatra, J., Wei, K., Liu, J. P. & Sun, S. Magnetic nanoparticles: Synthesis, Anisotropy, and applications. *Chem. Rev.* **123**, 3904–3943 (2023).
34. Wang, S. et al. Magnetic nanostructures: rational design and fabrication strategies toward diverse applications. *Chem. Rev.* **122**, 5411–5475 (2022).
35. Nikseresht, A., Karami, M. & Mohammadi, M. Phosphotungstic acid-Supported hercynite: A magnetic nanocomposite catalyst for the selective esterification of chloroacetic acid. *Langmuir* **40**, 18512–18524 (2024).
36. Liu, B. & Zhang, Z. Catalytic conversion of biomass into chemicals and fuels over magnetic catalysts. *ACS Catal.* **6**, 326–338 (2016).
37. Kilic, A. & Soylemez, R. Various in vitro and in vivo current biomedical applications of metal oxide nanoparticles (MO NPs) from synthesis to spectroscopic studies: a brief review. *Biochem. Biophys. Res. Commun.* **786**, 152747 (2025).
38. Kilic, A., Emin Karatas, M., Beyazsakal, L. & Okumus, V. Preparation and spectral studies of boronate ester modified magnetite iron nanoparticles (Fe3O4@APTES-B) as a new type of biological agents. *J. Mol. Liq.* **361**, 119602 (2022).
39. Wang, D. & Astruc, D. Fast-growing field of magnetically recyclable nanocatalysts. *Chem. Rev.* **114**, 6949–6985 (2014).
40. Kilic, A., Gezer, E., Durap, F., Aydemir, M. & Baysal, A. Pd(II) supported Dioxime functionalized Fe3O4 nanoparticles as efficient, eco-friendly and reusable catalysts for the Suzuki-Miyaura cross-coupling reaction in water. *J. Organomet. Chem.* **896**, 129–138 (2019).
41. Hasan, K., Shehadi, I. A., Joseph, R. G., Patole, S. P. & Elgamouz, A. β-Cyclodextrin-Functionalized Fe3O4-Supported Pd-Nanocatalyst for the reduction of nitroarenes in water at mild conditions. *ACS Omega.* **8**, 23901–23912 (2023).

42. Danehchin, M. & Esmaeili, A. A. Synthesis of Fe3O4@SiO2@Pr-NH2@DAP as a magnetic recyclable nano-catalyst for efficient synthesis of Pyranothiazolopyrimidines and 4H-pyrans under solvent-free condition. *Sci. Rep.* **13**, 14937 (2023).
43. Alnuwaiser, M. A. et al. Nanomagnetic 4-amino-3-hydroxynaphthalene-1-sulfonic as an efficient heterogeneous catalyst for multicomponent synthesis of 2-amino-3-cyano-4,6-diarylpyridines under green conditions. *Sci. Rep.* **15**, 40058 (2025).
44. Rezayati, S. et al. Magnetic Silica-Coated picolylamine copper complex [Fe3O4@SiO2@GP/Picolylamine-Cu(II)]-Catalyzed Biginelli annulation reaction. *Inorg. Chem.* **61**, 992–1010 (2022).
45. Bojabady, F., Kamali-Heidari, E. & Sahebian, S. Hydrothermal synthesis of highly aligned Fe3O4 nanosplates on nickel foam. *Mater. Chem. Phys.* **305**, 127828 (2023).
46. Mondal, J., Gomes, R., Modak, A. & Bhaumik, A. Pd-anchored functionalized mesoporous materials as robust and recyclable heterogeneous catalysts for a series of C-C bond forming reactions. *Recycl. Catal.* **1**, 10–33 (2013).
47. Trujillo, S. A., Peña-Solórzano, D., Bejarano, O. R. & Ochoa-Puentes, C. Tin(ii) chloride dihydrate/choline chloride deep eutectic solvent: redox properties in the fast synthesis of: N -arylacetamides and indolo(pyrrolo)[1,2- a] quinoxalines. *RSC Adv.* **10**, 40552–40561 (2020).
48. Zhao, Y. et al. Effect of nanoporous structure on the catalytic activity of nanoporous palladium for hydrogenation of nitro compounds. *ChemistrySelect* **5**, 7086–7092 (2020).
49. Dasgupta, H. R., Mukherjee, S. & Ghosh, P. A novel approach towards chemoselective reduction of nitro to amine. *Tetrahedron Lett.* **60**, 151028 (2019).
50. Dai, Z. et al. Michael addition reaction catalyzed by imidazolium chloride to protect amino groups and construct medium ring heterocycles. *Molecules* **24**, 4224 (2019).
51. Kale, A., Medishetti, N., Kanugala, S., Ganesh Kumar, C. & Atmakur, K. Na2S-promoted reduction of Azides in water: synthesis of pyrazolopyridines in one pot and evaluation of antimicrobial activity. *Org. Biomol. Chem.* **17**, 3186–3194 (2019).
52. Guilarte, V., Castroviejo, M. P., García-García, P., Fernández-Rodríguez, M. A. & Sanz, R. Approaches to the synthesis of 2,3-dihaloanilines. Useful precursors of 4-functionalized-1 H-indoles. *J. Org. Chem.* **76**, 3416–3437 (2011).
53. Avyyangar, N. R., Kalkote, U. R., Lugade, A. G., Nikrad, P. V. & Sharma, V. K. Partial reduction of dinitroarenes to nitroanilines with hydrazine hydrate. *Bull. Chem. Soc. Jpn.* **56**, 3159–3164 (1983).
54. Borah, H. N., Prajapati, D. & Boruah, R. C. Bakers' yeast-catalyzed ring opening of benzofuroxans: an efficient green synthesis of aryl-1,2-diamines. *Synth. Commun.* **39**, 267–272 (2009).
55. Iranpoor, N. & Panahi, F. Direct Nickel-Catalyzed amination of phenols via CO bond activation using 2,4,6-Trichloro-1,3,5-triazine (TCT) as reagent. *Adv. Synth. Catal.* **356**, 3067–3073 (2014).
56. Carlier, L., Baron, M., Chamayou, A. & Couarraze, G. Use of co-grinding as a solvent-free solid state method to synthesize dibenzophenazines. *Tetrahedron Lett.* **52**, 4686–4689 (2011).
57. Rafiee, F. & Shirzadi, F. The synthesis and characterization of a magnetic histidine schiff base palladium complex and its efficiency investigation in the nitroarene pollutants reduction and dyes degradation. *Appl. Organomet. Chem.* **36**, e6582 (2022).
58. Zeynizadeh, B., Mohammad Aminzadeh, F. & Mousavi, H. Green and convenient protocols for the efficient reduction of nitriles and nitro compounds to corresponding amines with NaBH4 in water catalyzed by magnetically retrievable CuFe2O4 nanoparticles. *Res. Chem. Intermed.* **45**, 3329–3357 (2019).
59. Liu, C. C. et al. Secondary phosphine Oxide-Stabilized Pd nanoparticles: Ligand-Controlled chemoselective hydrogenation of nitro compounds toward amines in water. *ACS Omega.* **10**, 24071–24078 (2025).
60. Jia, W. G. et al. Half-Sandwich ruthenium complexes with Schiff-Base ligands: Syntheses, Characterization, and catalytic activities for the reduction of nitroarenes. *Organometallics* **35**, 503–512 (2016).

Acknowledgements

This article is derived from a research grant funded by the Research, Development, and Innovation Authority (RDIA) - Kingdom of Saudi Arabia - with grant number (12615-iu-2023-IU-R-2-1-EI-).

Author contributions

Ammar Yasir Ahmed: ** Conceptualization, Investigation, Data curation, Validation, Visualization.Hamad AlMohamadi: ** Conceptualization, Supervision, Methodology, Investigation, Formal analysis, Writing – review & editing, Project administration.**Hazem Saed Zabibah: ** Writing - Review & Editing, Software.**Subbulakshmi Ganesan: ** Investigation, Methodology, Data curation, Formal analysis, Project administration support.**Vimal Arora: ** Investigation, Resources, Software, Writing – original draft.**Krithiga Thangavelu: ** Investigation, Formal analysis.**Pusparaj Samantsinghar: ** Writing - Review & Editing, Software.**Hamza Fadhel Hamzah and Basim Mohammed Saadi: ** Software, Resources, Data curation, Writing – review & editing.**Yasser Fakri Mustafa: ** Funding acquisition, Conceptualization, Supervision, Methodology, Writing – review & editing.

Declarations

Competing interests

The authors declare no competing interests.

Additional information

Correspondence and requests for materials should be addressed to A.Y.A. or H.A.